

C. Walldal  
S. Wall

## Coil-to-globule-type transition of poly(*N*-isopropylacrylamide) adsorbed on colloidal silica particles

Received: 14 December 1999  
In revised form: 22 February 2000  
Accepted: 6 March 2000

**Abstract** The temperature dependence of the dimensions of poly(*N*-isopropylacrylamide) (PNIPAM) adsorbed on two different colloidal silica particles was studied with dynamic light scattering. The hydrodynamic diameter was measured when the temperature was varied stepwise from 10 to 60 °C. PNIPAM molecules free in solution undergo a conformational transition at the  $\theta$  temperature. We have found that PNIPAM adsorbed onto silica particles also undergoes a transition below the  $\theta$  temperature. When a small amount of polymer was adsorbed the coil-to-globule transition at the  $\theta$  temperature did not occur. Potentiometric titrations showed that the surface charge of the silica particles was not affected by the polymer adsorption. Sodium dodecyl sulfate (SDS) (100–1200 mg/l) was added to improve the stability. The particles with a higher zeta potential required a smaller addition of SDS to prevent coagulation compared to the parti-

cles with a smaller surface potential. For low additions of SDS the transition curves of adsorbed PNIPAM were unaffected. For larger additions of SDS the collapse of PNIPAM was shifted to higher temperatures. When as much as 1200 mg/l SDS was added, two regions with weak transitions were observed before the collapse. It was also observed that the presence of SDS results in a smaller adsorption of PNIPAM onto the particles. The addition of SDS strongly increased the magnitude of the electrophoretic mobility of the polymer–particle unit. From the electrophoretic measurements an electrokinetic layer thickness was calculated and it was found to be smaller than the corresponding hydrodynamic layer thickness, as obtained by dynamic light scattering.

**Key words** Poly(*N*-isopropylacrylamide) · Silica particles · Coil-to-globule transition · Hydrodynamic thickness

---

C. Walldal (✉) · S. Wall  
Department of Physical Chemistry  
Göteborg University  
412 96, Göteborg, Sweden  
e-mail: charlott@phc.chalmers.se  
Tel.: +46-31-7722815  
Fax: +46-31-167194

### Introduction

The use of both natural and synthetic polymers to control the stability behaviour of colloidal suspensions has attracted much attention due to their considerable technological importance. In many technological applications a stable dispersion is desired first, followed by subsequent aggregation. Poly(*N*-isopropylacrylamide)

(PNIPAM) with a lower critical solution temperature at about 32 °C is therefore interesting to study.

Macromolecules can exist in several different conformations. In a good solvent there is a repulsion between the polymer segments which tends to expand the coil conformation. In a poor solvent, under worse than  $\theta$  conditions, the mean force acting between the segments becomes attractive and the polymer chains collapse. This

contraction (coil-to-globule transition) results in a space-filling globular conformation [1]. The physical properties of free polymers change when they adsorb onto a surface. An adsorbed chain also undergoes conformational changes even though the conformational transitions differ from those of free chains.

The coil-to-globule transition can be induced by changing the temperature to the worse-than- $\theta$ -solvent domain by adding a co-nonsolvent or by adding different kinds of polymers and oligomers to a dilute polymer solution and to gels [2, 3]. The coil-to-globule transition has been investigated for a few polymers. One of them is PNIPAM, which undergoes chain collapse when the water temperature is increased to 31–34 °C, whereupon the PNIPAM molecules coagulate [4, 5]. The collapse temperature is independent of molecular weight. The collapse is generally thought to result from changes in hydrogen bonding and hydrophobic interactions both within and between the segments of the PNIPAM chains and the solvent water molecules. To prevent aggregation of the polymer chains during the coil-to-globule transition a small amount of surfactant can be added which adsorbs onto the polymer chains, leading to electrostatic repulsion among the polymer segments [6–8]. The interaction of sodium dodecyl sulfate (SDS) with microgel particles has also been studied [9, 10].

An alternative way to study the coil-to-globule transition is to adsorb or graft the polymer chains onto latex particles [11–13], which are thus electrosterically stabilised. Upon increasing the temperature a second transition of the attached polymer chains under better than  $\theta$  conditions is observed [12]. This second transition has been interpreted as an  $n$ -cluster formation as proposed by de Gennes [14]. The  $n$ -cluster concept postulates the formation of intramolecular clusters of hydrophobic moieties. Below the  $\theta$  temperature the  $n$ -cluster formation is absent for polymers free in solution because of the low density of polymer segments.

The amount of PNIPAM adsorbed on silica particles as a function of temperature has been studied by Tanahashi et al. [15]. They found that the amount of PNIPAM adsorbed increased with temperature for both hydrophobic and hydrophilic silica.

Electrophoretic mobility and viscosity measurements have previously been used as two independent methods to determine the segment density distribution of an adsorbed polymer [16]. The electrokinetic thickness of an adsorbed neutral polymer depends on the ionic strength and the nature of the polymer, whereas the hydrodynamic diameter only depends on the adsorbed neutral polymer.

In this study PNIPAM is adsorbed onto negatively charged colloidal silica particles. The hydrodynamic diameter was measured with dynamic light scattering

(DLS). SDS was added to improve the stability. SDS forms micelles with the free PNIPAM chains at a critical aggregation concentration (cac) of 230 mg/l [17]. Even a very small amount of SDS is sufficient to improve the stability and prevent aggregation, facilitating observation of the coil-to-globule transitions [7]. From the electrophoretic mobility measurements the zeta potential and the electrokinetic layer thickness were calculated. The latter was compared to the hydrodynamic layer thickness as obtained from DLS.

Finally, a potentiometric titration was also performed on the silica particles with and without adsorbed PNIPAM.

## Materials and methods

### Poly(*N*-isopropylacrylamide)

In this study both fractionated and unfractionated samples of PNIPAM were used. NIPAM was purified by recrystallisation from a 65/35 mixture of hexane and benzene. Potassium peroxydisulfate ( $K_2S_2O_8$ , BDH Chemicals) and sodium metabisulfite ( $Na_2S_2O_5$ , Merck) were used as received. 2,2'-Azobis(isobutyronitrile) (AIBN, Fluka) was recrystallised from alcohol. Millipore Milli-Q water was used.

### Unfractionated PNIPAM

NIPAM (2 g) was polymerised in water (100 g) at room temperature using potassium persulfate (KPS) (1.2%  $K_2S_2O_8$  of the NIPAM weight) and  $Na_2S_2O_5$  (0.5 mole of the amount of KPS added) as an initiator under a nitrogen atmosphere. The sample was filtered and dialysed by repeated changes of fresh Millipore Milli-Q water. The weight-average molecular weight was calculated, with data obtained by light scattering using a Zimm plot, to be  $1.2 \times 10^6$  g/mol in water at 25 °C.  $M_w/M_n$  was approximately 10 according to gel permeation chromatography analysis, which also revealed that the size distribution exhibited a slight bimodality. The radius of gyration was 60 nm.

### Fractionated PNIPAM

NIPAM (10 g) was polymerised for about 20 h at 65 °C in a 70/30 benzene/acetone mixture (100 g) using AIBN (1%) as the initiator under a nitrogen atmosphere. The solvents were then evaporated in vacuum at room temperature. The molecular-weight fractionation of PNIPAM was performed in a two-phase system of acetone/*n*-hexane at room temperature. Both the acetone and *n*-hexane were carefully dried. The average molecular weight of the first fractionated PNIPAM was found to be  $1.2 \times 10^6$  g/mol as measured by light scattering in water at 25 °C.

### Colloidal silica particles

Two different monodisperse colloidal silica particle (CSA) systems were used. The smaller particles were a gift from Eka Chemicals and the larger particles were a gift from Peter Greenwood, Department of Engineering Chemistry, Chalmers University of Technology. The diameters were 21 nm (determined from the Brunauer–Emmett–Teller adsorption isotherm) and 80 nm (determined from scanning electron microscopy and sedimentation, Horiba Capa-700), respectively.

The dynamic mobility of the silica particles suspended in 2 mM NaCl was measured with an Acoustosizer and the mobility values were fitted using Mangelsdorf and White's [18] computer program for determining the zeta potentials. The larger silica particle, 80 nm, was found to exhibit an unusually high zeta potential of  $-145 \pm 15$  mV, whereas the smaller particle had a zeta potential of  $-100 \pm 10$  mV.

#### Sample preparation

A constant amount of silica (0.0028 g/ml) was added to different amounts of PNIPAM and the samples were left for 24 h to equilibrate. The samples were centrifuged and the free nonadsorbed polymer was removed before the measurements. The conductivity of the samples was approximately 300  $\mu\text{S}/\text{cm}$  and the pH was about 9. In all experiments Millipore Milli-Q water was used and all samples were filtered using 0.45- $\mu\text{m}$  Millipore filters before the measurements. The unfractionated PNIPAM was used in the experiments if nothing else is stated.

#### Dynamic light scattering

DLS measurements of the polymer-coated particles were performed at a particle concentration of  $4 \times 10^{-5}$  g particles/g solvent with an argon ion laser ( $\lambda = 488$  nm) operating at a scattering angle of 90° with a power of 150 mW. The autocorrelation function,  $G(\tau)$ , was measured using a Malvern 4700c correlator. The hydrodynamic diameters were calculated using the Stokes-Einstein equation, with the values of the viscosity and the refractive indexes taken from the literature [19]. During an experiment the temperature was increased stepwise from 10 to 60 °C. The estimated error of the hydrodynamic diameter was  $\pm 4$  nm at the most.

#### Surface charge density

Potentiometric titrations were performed at 25 °C using a Radiometer PHM 82. The sample (20 ml) was equilibrated in a nitrogen atmosphere for 40 min before the titration was initiated. Different amounts of the 80-nm silica particles (2, 6 and 12% weight concentrations) were used initially and similar charge densities were obtained. Therefore, a 2% particle dispersion was used for the titration experiments of the PNIPAM-covered particles due to the smaller amount of polymer needed. The titrations were started at pH 9.5, and 50 mM HCl was added in portions of 0.01 ml to the samples via an autoburette. A similar titration of the background electrolyte (5 mM NaCl) was also performed. The volume of acid required to lower the pH for the background electrolyte was subtracted from the volume of acid needed to lower the pH for the silica particles. The dissolution of silica was corrected for following the method of Alexander et al. [20].

#### Electrophoretic mobility

A Malvern Zetasizer was used for the electrophoretic mobility measurements. The measurements were performed on particles with different amounts of PNIPAM adsorbed and also on particles with a constant amount of PNIPAM and different SDS concentrations. Mobility measurements were also performed on bare silica particles with and without added SDS. The 80-nm particles were used at a concentration of 0.005 g particles/ml sample and the samples were prepared as previously described. The temperature was maintained at 25 °C; the pH was adjusted to 9 and the ionic strength was 5 mM NaCl for the PNIPAM/CSA samples. When SDS was added to the samples the total ionic strength was adjusted to 5 mM by adding the proper amount of NaCl. The zeta

potentials and the surface charges were calculated from the electrophoretic mobilities using the computer program "Mac Mobility", which is based on O'Brien and White's theory [21].

## Results

#### Dynamic light scattering

The diameter at 10 °C for different amounts of fractionated PNIPAM added to the 80-nm particles is shown in Fig. 1. PNIPAM is assumed to adsorb onto the silica surface through hydrogen bonding between the polymer and the silanol groups. In Fig. 1 it is seen that the hydrodynamic diameter increases as more PNIPAM is added. This demonstrates that the polymer adsorbs on the particles and that the polymer conformation becomes increasingly extended as more PNIPAM is adsorbed. At 4 g PNIPAM/g CSA a plateau is reached. At this point the thickness of the adsorbed polymer layer is about 125 nm.

The hydrodynamic diameter of the two different particles with the same amount of PNIPAM added (1 g added PNIPAM/g CSA) is shown as a function of temperature in Fig. 2. As seen, the extension of the adsorbed polymer layer decreases as the temperature increases. Above 33 °C, when passing into the worse-than- $\theta$ -solvent regime, the particles coagulate, which is shown by an increased particle size and irreproducible results. At 10 °C the extension of the adsorbed polymer

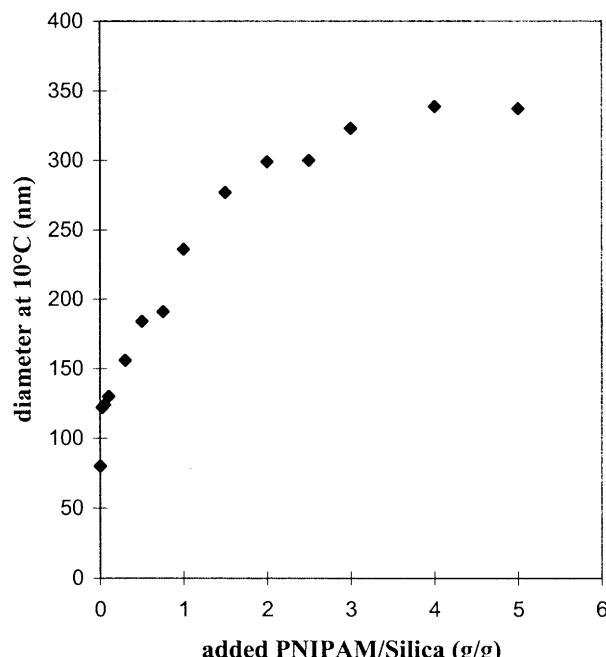


**Fig. 1** The hydrodynamic diameter of poly(*N*-isopropylacrylamide) (PNIPAM)-covered silica particles (80 nm) at 10 °C versus different amounts of added PNIPAM/g colloidal silica particles (CSA)

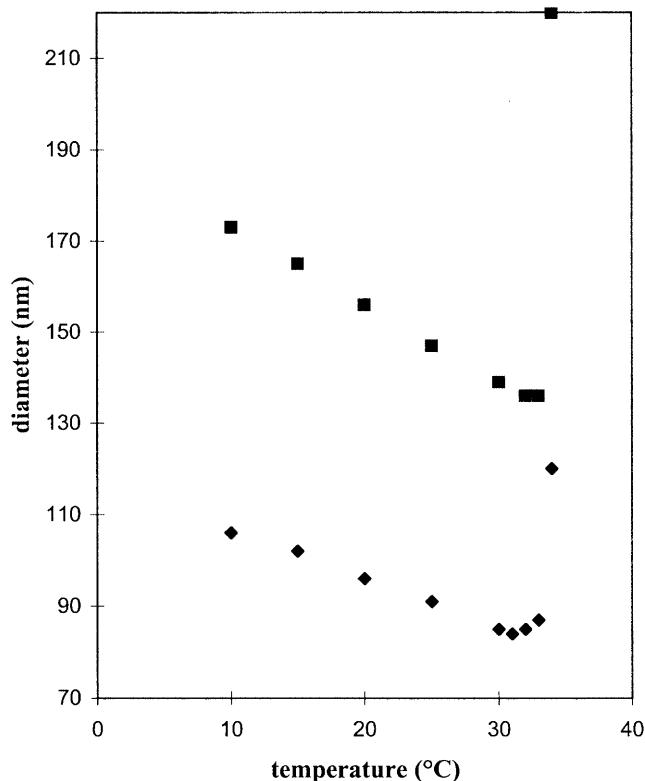


Fig. 2 The hydrodynamic diameter of the 21-nm (◆) and the 80-nm (■) particles with 1 g added PNIPAM/g CSA versus temperature

layer was 47 nm for the 80-nm particles and 43 nm for the 21-nm particles. When the temperature was increased from 10 to 32 °C the total change in the polymer adlayer thickness was 22 nm for the 21-nm particles and 37 nm for the 80-nm particles.

The temperature dependence of the hydrodynamic diameter when 4 g PNIPAM/g CSA is adsorbed on the 80-nm particles is shown in Fig. 3. The polymer layer is very extended due to the large amount of PNIPAM added. In changing the temperature from 10 to 20 °C the polymer layer thickness changes by 80 nm in total. However, such a large change is not observed when the temperature is increased from 20 to 33 °C; then the reduction of the layer is only 15 nm and at 34 °C the particles aggregate.

In Fig. 4, the situation where a smaller amount of polymer has been added, 0.1 g PNIPAM/g CSA, to the 21-nm particles is illustrated. As expected, this results in a smaller extension of the adsorbed polymer layer than previously. The decrease in the polymer layer when heating from 10 to 60 °C is small but significant, and no aggregation is observed. In Fig. 4 it is also shown that the addition of 10 mM NaCl to a similar sample reduces the stability. When passing into bad solvent conditions coagulation takes place. Another observation connected with the addition of 10 mM NaCl is that

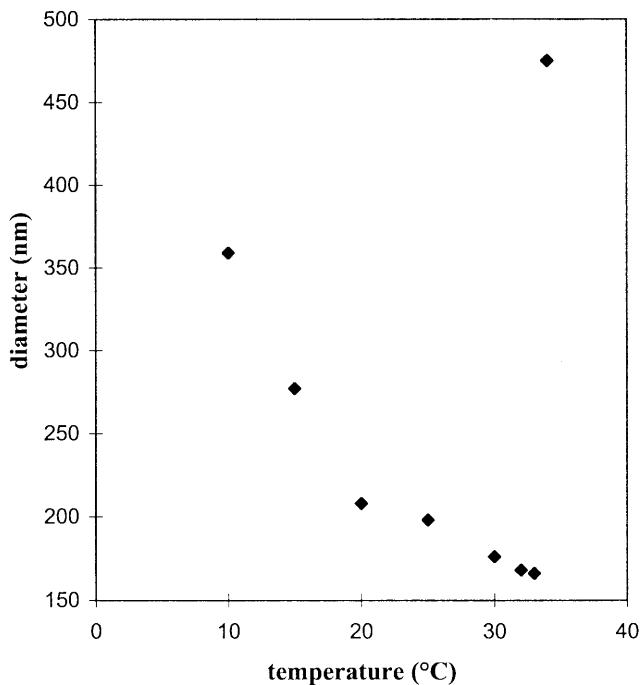


Fig. 3 The hydrodynamic diameter of 4 g added PNIPAM/g CSA (80 nm) versus temperature

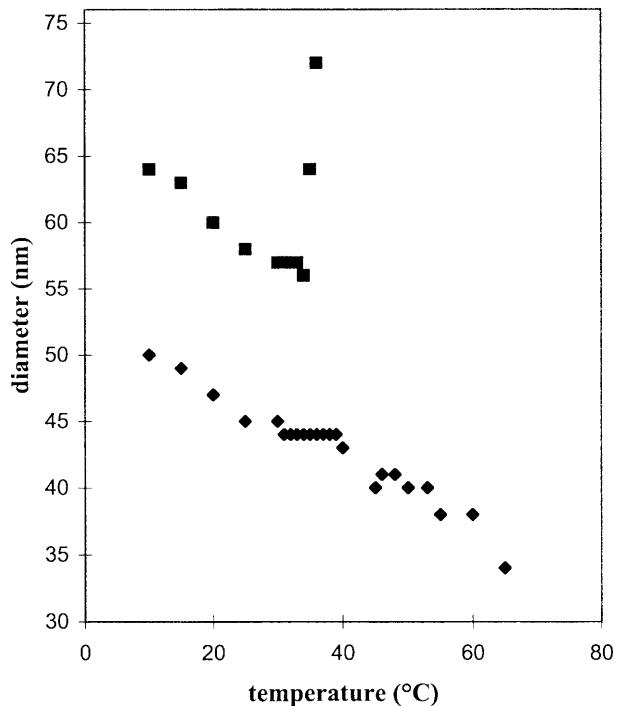


Fig. 4 The hydrodynamic diameter of 0.1 g PNIPAM/g CSA (21 nm) without added NaCl (◆) and with 10 mM NaCl (■) versus temperature

the extension of the polymer layer increases by about 10 nm at 10 °C.

In Fig. 5 one sample with unfractionated polymer and another sample with fractionated polymer (both with 0.05 g PNIPAM/g CSA) are shown as a function of temperature. Apart from the fractionated sample giving a larger hydrodynamic diameter, the two samples behaved similarly. Both polymer layers decreased up to 38 °C and no coagulation was observed.

#### Addition of SDS

The initial diameters at 10 °C of the two different particle dispersions used are shown for 1 g PNIPAM/g CSA as the SDS concentration was increased in Fig. 6. At low SDS concentrations (below 300 mg/l) the change in the diameter is small and within the experimental errors. At higher SDS concentrations there is a decrease in the initial diameter. It can also be observed that the thickness of the adsorbed PNIPAM layer at 10 °C is about the same for the two different particles even when the amount of SDS increases.

Figure 7 illustrates the situation where 150 mg/l SDS was added to the 80-nm particles with 1 g PNIPAM/g CSA added. The initial diameter at 10 °C and the resulting layer reduction up to 33 °C are comparable in magnitude to a similar sample without SDS (Fig. 2). Between 33 and 35 °C a strong transition is seen in

Fig. 7 and the resulting polymer layer is found to be nearly flat. The total decrease in the hydrodynamic diameter is 85 nm.

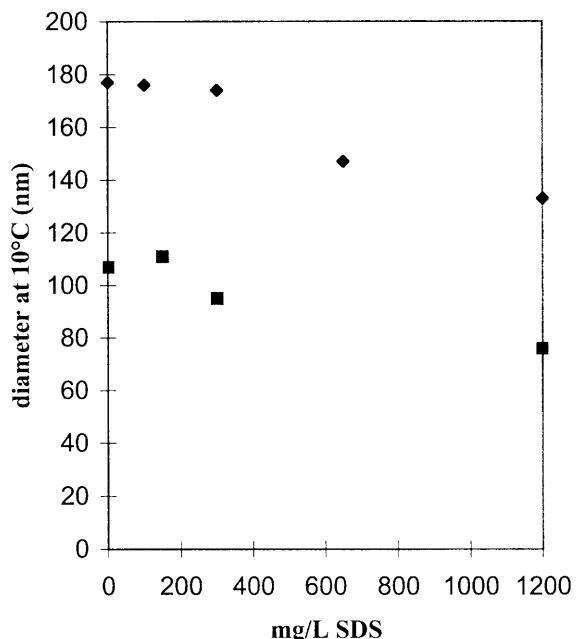


Fig. 6 The hydrodynamic diameter at 10° of 1 g PNIPAM/g CSA for both 80-nm (◆) and 21-nm (■) particles versus amount of sodium dodecyl sulfate (SDS) added

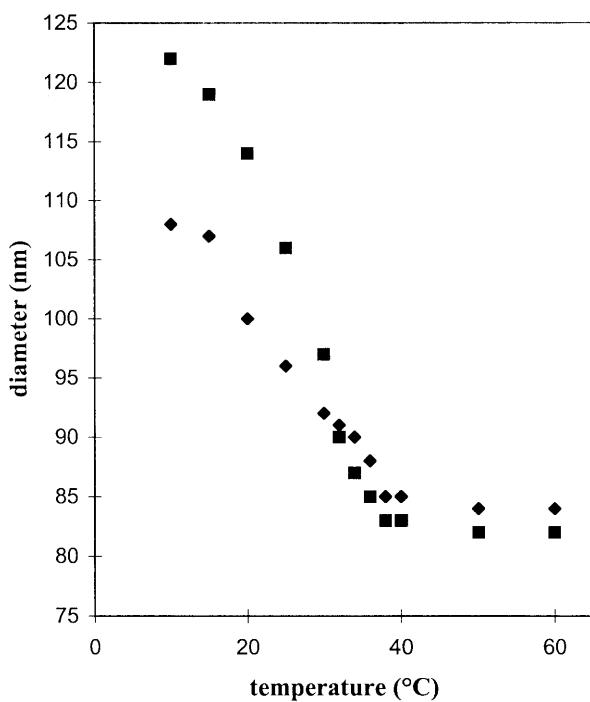


Fig. 5 The hydrodynamic diameter of fractionated (■) and unfractionated (◆) 0.05 g PNIPAM/g CSA (80 nm) versus temperature

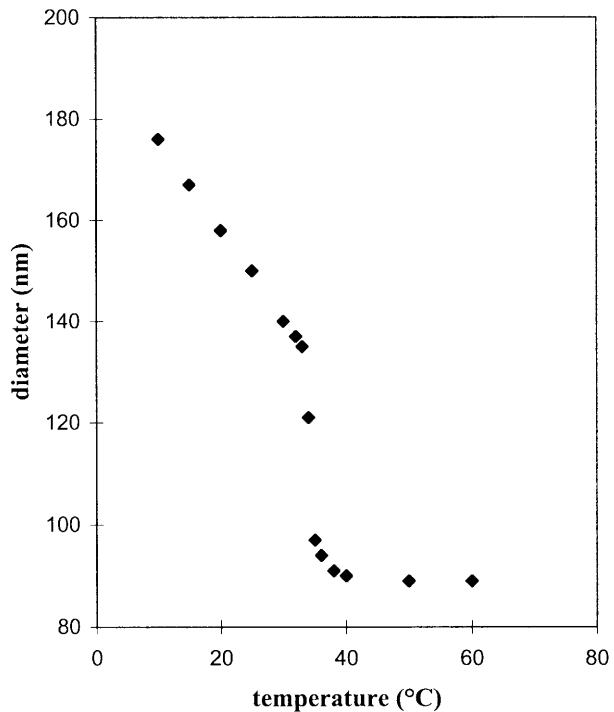


Fig. 7 The hydrodynamic diameter of 1 g PNIPAM/g CSA (80 nm) with 150 mg/l SDS versus temperature

The situation where 1200 mg/l SDS was added to the 21-nm particles is illustrated in Fig. 8 and the start of a major transition can be seen at 40 °C. At temperatures below 40 °C, a weaker transition is observed. Similar

observations were also made for the 80-nm particles (not shown here).

#### Surface charge densities

For a negatively charged surface we can write

$$\sigma_0 = -F(\Gamma_{\text{H}^+} - \Gamma_{\text{OH}^-}) = F([\text{H}^+](X - v)/mA , \quad (1)$$

where  $F$  is the Faraday constant,  $\Gamma_{\text{H}^+}$  and  $\Gamma_{\text{OH}^-}$  are the adsorption densities of  $\text{H}^+$  and  $\text{OH}^-$ , and  $[\text{H}^+]$  is the concentration of acid.  $X$  is the total amount of  $\text{HCl}$  added and  $v$  is the volume of acid required to change the pH of the silica by a certain amount.  $A$  is the surface area per unit mass of solids and  $m$  is the mass of the silica sample.

The surface charge of the silica particles with and without polymer adsorbed is plotted against pH in Fig. 9 for a volume fraction of 2%. There is a steep rise in surface charge above pH 9 even though the solubility of silica has been corrected for [22, 23]. The high surface charge is probably due to the porous structure of the silica particles used [24]. Titrations of two samples with different polymer concentrations (0.25 and 2 g PNIPAM/g CSA) required the same amount of acid to arrive at the same pH. At pH 9 this amount of acid was almost the same as for the bare particles. We assume, therefore, that the surface charge is more or less unaffected by the presence of PNIPAM at pH 9. The point of zero charge was assumed to be 3. The determination of surface charge becomes increasingly difficult with decreasing pH.

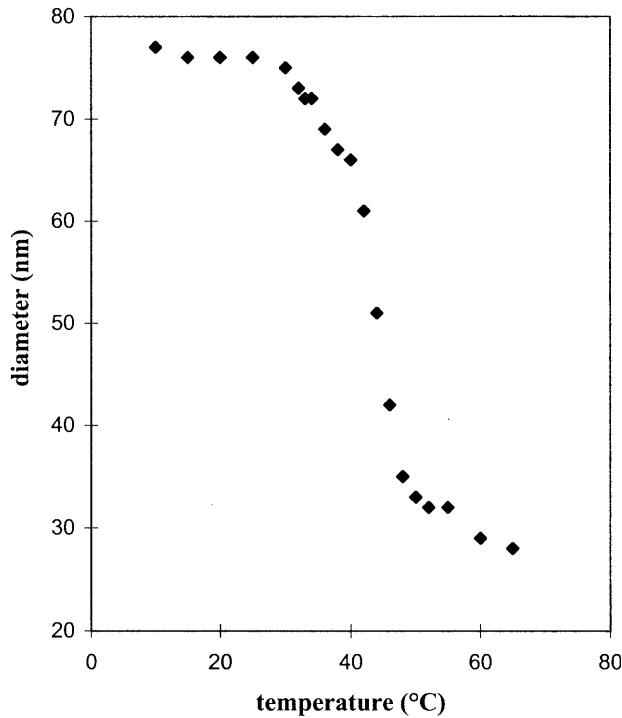
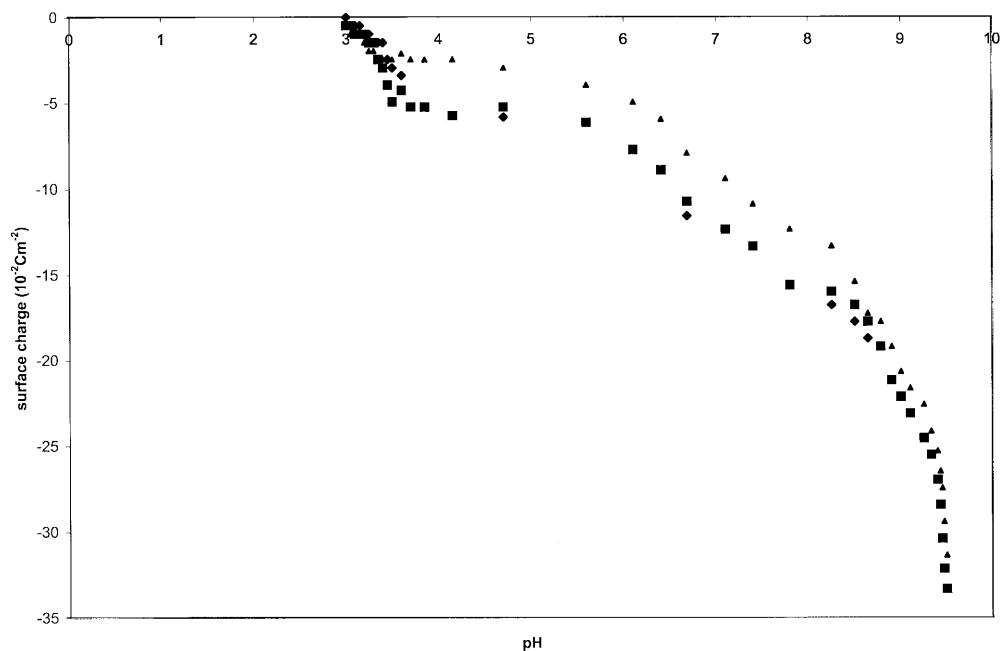


**Fig. 8** The hydrodynamic diameter of 1 g PNIPAM/g CSA (21 nm) with 1200 mg/l SDS versus temperature

**Fig. 9** The surface charge of bare 80-nm CSA ( $\blacktriangle$ ), CSA with 0.25 g PNIPAM ( $\blacklozenge$ ), and CSA with 2 g PNIPAM ( $\blacksquare$ ) versus pH



## Mobility measurements

The silica surface is negatively charged and is considered to be nonhydrophobic, so adsorption of SDS directly on the silica surface is not expected. This was confirmed by mobility measurements, in which the same silica sample with and without SDS added, but with a constant ionic strength, gave the same mobility value.

The electrophoretic mobility is shown for the 80-nm particles (pH 9 and 5 mM NaCl) with different amounts of PNIPAM added to a constant number of particles in Fig. 10. With increasing amount of PNIPAM the mobility decreases in magnitude. The mobility is already substantially reduced for 0.1 g PNIPAM/g CSA (from  $-3.6 \times 10^{-8} \text{ m}^2/\text{Vs}$  for the bare particle), and somewhere between 1 and 2 g PNIPAM/g CSA the mobility is reduced to zero. Samples with lower concentrations of PNIPAM were also prepared, but the samples were found to have coagulated slightly before the measurement. After filtering there was not a sufficient amount of material left to perform an electrophoretic measurement. The samples had been prepared at the lowest concentrations possible to avoid particle collisions, which could result in coagulation. This problem was not present in preparing samples for the DLS due to the smaller particle concentration needed compared to electrophoretic light scattering.

The electrophoretic mobility for the 80-nm particles with 1 g PNIPAM/g CSA is plotted against SDS concentration in Fig. 11. The electrophoretic mobility does not increase in proportion to the increased SDS concentration: instead two regions are observed.

The change in the position of the shear plane from the surface was calculated using [16]

$$\tanh(e\zeta/4kT) = \tanh(e\Psi_d/4kT) \exp[-\kappa(\Delta - \delta)], \quad (2)$$

which assumes that the Poisson–Boltzmann equation is valid outside the Stern plane (located a distance  $\delta$  from the surface). The shear plane is present at a distance  $\Delta$  from the surface,  $\zeta$  is the zeta potential, and  $\Psi_d$  denotes the potential at the outer Helmholtz plane (OHP).

For the bare silica particle it is assumed that  $\zeta = \Psi_d$ . Since the surface charge is almost the same for particles with and without adsorbed polymers, the potential at the OHP is assumed to be the same in the different samples.

For 0.25 g PNIPAM/g CSA the distance to the shear plane obtained with Eq. (2) was 13 nm with  $\delta = 4 \text{ \AA}$ . For 1 g PNIPAM/g CSA the distance was 16 nm and for zero mobility (zeta potential set to 0.5 mV) 20 nm. For comparison, the Debye length ( $1/\kappa$ ) is 4.3 nm in 5 mM NaCl.

The 16-nm electrokinetic layer obtained for 1 g PNIPAM/g CSA can be compared to the 35-nm hydrodynamic layer as obtained with DLS (Fig. 2). As expected the electrokinetic layer is smaller than the hydrodynamic layer.

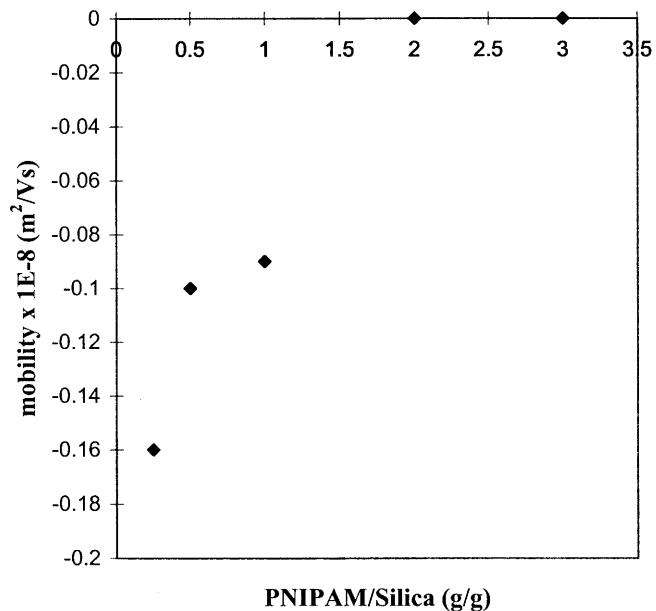


Fig. 10 The mobility versus different amounts of PNIPAM/CSA

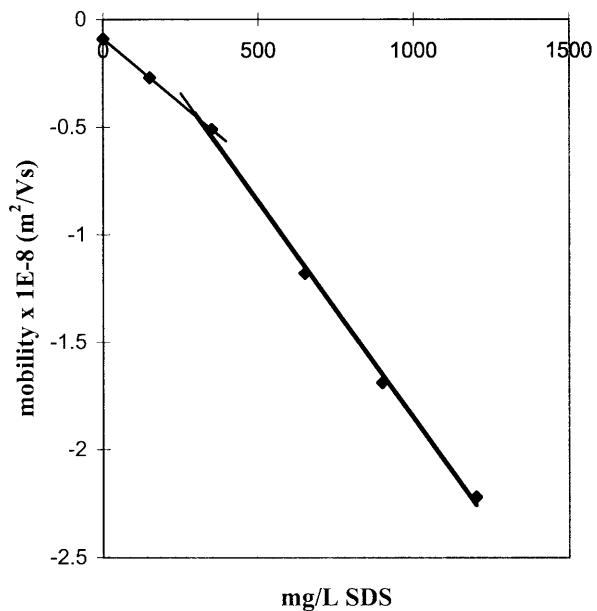


Fig. 11 The mobility of 1 g PNIPAM/g CSA versus SDS concentration

## Discussion

PNIPAM adsorbed onto silica particles undergoes a coil-to-globule transition at the  $\theta$  temperature. The size of the polymer layer also decreased substantially in the temperature region 10–34 °C due to attractive forces in the polymer layer, leading to a contraction of the polymer chains. The shrinkage of the polymer layer may be due to

the hydrophobic attraction between the isopropyl moieties attached to the polymer backbone, as well as hydrogen-bond formation. With increasing temperature the hydrogen bonding with water is increasingly disrupted. The attraction between the polymer segments is enhanced and there is a size reduction of the polymer layer. Since the total system is stable, the attraction is apparently not sufficiently strong to coagulate the polymer-covered particles. Below the  $\theta$  temperature the particles are electrosterically stabilised. At the  $\theta$  temperature the steric repulsion originating in the outer part of the polymer layer is replaced by an attractive force between the polymers adsorbed on different particles.

Due to the simultaneous observation of steric stabilisation and the coil-to-globule transition below the  $\theta$  temperature, the  $n$ -cluster formation seems to be a plausible mechanism as proposed by de Gennes [25]. The attraction leads to the formation of a cluster consisting of  $n$  segments [12]. According to the theoretical prediction [26], the  $n$ -cluster formation occurs in the denser parts of the polymer layer close to the interface. It is the outer, less dense region of the structured interfacial layer that imparts the steric stabilisation. This is predicted to occur in solvents that are better than  $\theta$  solvents.

Another interesting aspect is to compare the effect of having particles of different size. A comparison of the initial thickness at 10 °C of the 21-nm and 80-nm particles shows about the same thickness of the adsorbed polymer layers; however, when the temperature was increased there was a larger decrease in the adsorbed polymer layer on the 80-nm particle than on the 21-nm particle. At 10 °C, the volume of the adsorbed polymer layer was about 8 times larger for the 80-nm than the 21-nm particles (Fig. 2); however, at 32 °C the volume of the polymer layer was only twice as large for the larger particles.

Several investigations [26–30] have found that the extension of the polymer layer steadily increases with increasing particle radius. Baker et al. [29] concluded that particles of smaller radii allow polymer segments greater access to the particle surface, which results in a higher segment density close to the surface but a lower adlayer thickness. According to this view a larger amount of polymer should be adsorbed on the 21-nm particles than on the 80-nm particles to maintain the same polymer layer thickness. If this is correct it should result in a higher segment density around the smaller particles compared to around the larger ones. This would favour the  $n$ -cluster formation at the 21-nm particle surface. In contrast, however, it is the polymer layer on the larger particle surface which decreases the most with increasing temperature. This can be due to the fact that at 10 °C we already have a larger  $n$ -cluster formation at the smaller particle surface due to the higher segment density, which is caused by the larger curvature of the particle surface. There is also a

possibility for the 21-nm particle that the density of the outer polymer layer is high enough to prevent a part of the transition from occurring under better than  $\theta$  solvency conditions through steric hindrance.

A substantial decrease in the PNIPAM layer was observed (Fig. 3) up to 20 °C. As the temperature was further increased the decrease was less pronounced.

In the case shown in Fig. 4 the attractive force at the  $\theta$  temperature was not sufficiently strong (due to the small amount of PNIPAM) to overcome the electrostatic repulsion between the silica particles. Also, there is no large size reduction at the  $\theta$  temperature. Instead there is a small but constant decrease in the polymer layer in the temperature interval. Presumably strong interactions between the polymer and the surface prevent the coil from collapsing in worse than  $\theta$  solvents. The increased diameter obtained with increased ionic strength has no simple explanation. An explanation, albeit speculative, is if the solubility of PNIPAM decreases with increasing ionic strength, there could be enhanced adsorption from solution.

It has been reported that the critical solution temperature of PNIPAM in water is quite independent of both the molecular weight and the volume fraction of the polymer [4, 31]. This also seems to be a valid observation for the molecular weight of PNIPAM adsorbed onto silica particles; the results in Fig. 5, when both the fractionated and the unfractionated sample were used, show about the same layer thickness at 32 °C even though the layer thicknesses initially differed. This is due to the fact that the fractionated sample only includes the larger molecules, which in the unfractionated sample are mixed with the smaller ones.

There were two major effects in the DLS measurements by increasing the amount of SDS added. One was that the hydrodynamic diameter decreased and the other was that the transition temperature was elevated.

Added SDS adsorbs onto PNIPAM, which then becomes negatively charged. At a SDS concentration of 300 mg/l the coil size of free PNIPAM increases [6]. Following this, if the same amount of PNIPAM with and without SDS was adsorbed on the silica particles, the hydrodynamic diameter should be larger for the sample with SDS. The fact that the hydrodynamic diameter decreases as more SDS is added (Fig. 6) shows that a smaller amount of PNIPAM is actually adsorbed. This could be due to the electrostatic repulsion between the particle surface and PNIPAM with adsorbed SDS and between PNIPAM chains with adsorbed SDS. Jean et al. [8] studied the effects of SDS on the adsorption behaviour of PNIPAM at the air–water interface. They report that an increased amount of added SDS decreased the packing density of PNIPAM chains at the air–water interface. This finding supports our conclusion that less PNIPAM is adsorbed when the amount of SDS added is increased.

The other effect of adding SDS to the polymer-covered particles is that the transition temperature was elevated (observed at 650 mg/l added SDS but not at 300 mg/l). The transition was shifted to higher temperatures probably because of the increased repulsion between the ionic heads of the adsorbed SDS. For free PNIPAM molecules with adsorbed SDS the transition was already shifted to higher temperatures at 300 mg/l [6]. A possible explanation is that less SDS is adsorbed onto PNIPAM when the polymer is adsorbed on the negatively charged silica particles compared to when the same amount of PNIPAM is free in solution.

In Fig. 8 there is also a weaker transition at lower temperatures. This phenomenon has also been observed for PNIPAM chains attached to polystyrene latex particles [32]. The weaker transition, observed before the large transition at very high SDS concentrations, was attributed to the formation of ion pairs between the charges on PNIPAM–SDS complexes and counterions [32]. The ion pairs create cross-links which contract the polymer layer.

Another explanation could be that with increasing temperature more SDS adsorbs onto PNIPAM due to the decreased amount of water bound to the PNIPAM molecules [33]. The transitions are weaker due to increased adsorption of SDS until the attractive forces within the molecule chain become strong enough and a larger transition occurs. When large amounts of SDS are added this can have an effect on the transitions in better than  $\theta$  solvents.

Mylonas et al. [7] have shown that the aggregation number of the SDS aggregates on free PNIPAM molecules is about 7–8 surfactant molecules per aggregate when the SDS concentration is between 2.5–6 mM. Above these concentrations the aggregation number increases upon increasing the SDS concentration [7]. It is likely that this enhanced adsorption of SDS also occurs in a PNIPAM–particle–SDS system; however, as the SDS concentration in Fig. 8 is only 4.2 mM, it is uncertain whether it is an increase in the aggregation number compared to that observed in Fig. 7. We conclude that the effect observed in Fig. 8 is due to the increased adsorption of SDS.

The aggregation of the 21-nm particles could be prevented for SDS concentrations above 450 mg/l (not shown in the figure), whereas a small amount of SDS (150 mg/l) was sufficient to stabilise the 80-nm particles. This is in agreement with the higher zeta potential of the

80-nm particles as obtained from dynamic mobility measurements.

We have already concluded that adsorption of SDS onto PNIPAM decreases the amount of polymer adsorbed on the particles. This conclusion is supported by the mobility results in the following way. The increase in negative mobility can be due to an additional charge coming from the adsorbed SDS and/or the fact that the shear plane is moved closer to the surface when a smaller amount of polymer is adsorbed. The diameter at 25 °C for 1 g PNIPAM/g CSA (80 nm) and 1200 mg/l SDS (not shown) is about 135 nm, which is almost the same diameter as that measured at 10 °C (Fig. 6) due to a very weak transition. In Fig. 1 a diameter of about 135 nm corresponds to about 0.25 g added PNIPAM/g CSA at 10 °C with no SDS adsorbed. We have noted (Fig. 11) that adsorption of PNIPAM (0.25 g/g) onto silica particles without SDS gives a mobility of about  $-0.16 \times 10^{-8}$  m<sup>2</sup>/Vs. Since the mobility is  $-2.2 \times 10^{-8}$  m<sup>2</sup>/Vs when 1200 mg/l SDS is added, it can be concluded that there has to be both a decreased amount of polymer adsorbed and adsorption of SDS. The larger increase in the mobility above 350 mg/l added SDS (Fig. 11) could be due to both a larger adsorption of SDS onto the PNIPAM and a decreased adsorption of PNIPAM onto the particles. The increased adsorption of SDS is likely to be due to the formation of SDS micelles on the PNIPAM molecules.

## Conclusions

It has been shown that PNIPAM adsorbed onto CSA undergoes a coil-to-globule transition at the  $\theta$  temperature. A shrinkage of the PNIPAM layer was also observed under better than  $\theta$  solvency conditions, which is interpreted as an *n*-cluster formation. This shrinkage depended on the density of the polymer layer. The stability of the two different particle dispersions was in accordance with differences in the electrophoretic mobilities. Addition of SDS improved the stability of the polymer–particle units. SDS increased the magnitude of the electrophoretic mobility even below the cac.

**Acknowledgements** Don Napper is acknowledged for providing the opportunity to perform this work at the Department of Physical Chemistry, Sydney University, and for valuable comments and discussions. Peng Wei Zhu is acknowledged for making the PNIPAM, experimental assistance, and for valuable discussions.

## References

1. Fujita H (1990) Polymer solutions. Elsevier, New York
2. Tanaka F (1983) J Chem Phys 78:2788
3. Nose T (1986) J Phys 47:517
4. Binkert Th, Oberreich J, Meewes M, Nyffenegger R, Rica J (1991) Macromolecules 24:5806
5. Wu C, Zhou S (1995) Macromolecules 28:5388

6. Meewes M, Ricka J, de Silva M, Nyffenegger R, Binkert Th (1991) *Macromolecules* 24:5811
7. Mylonas Y, Staikos G, Lianos P (1999) *Langmuir* 15:7172
8. Jean B, Lee L-T, Cabane B (1999) *Langmuir* 15:7585
9. Tam KC, Ragaram S, Pelton RH (1994) *Langmuir* 10:418
10. Mears SJ, Deng Y, Cosgrove T, Pelton RH (1997) *Langmuir* 13:1901
11. Pelton RH (1988) *J Polym Sci Part A Polym Chem* 26:9
12. Zhu PW, Napper DH (1994) *J Colloid Interface Sci* 164:489
13. Zhu PW, Napper DH (1997) *J Phys Chem B* 101:3155
14. de Gennes P-G (1991) *CR Acad Sci Ser 2* 313:1117
15. Tanahashi T, Kawaguchi M, Honda T, Takahashi A (1994) *Macromolecules* 27:606
16. Fleer GJ, Koopal LK, Lyklema (1972) *Kolloid ZZ Polym* 250:689
17. Schild HG, Tirell DA (1989) *Polym Prep Am Chem Soc Div Polym Chem* 30:350
18. Mangelsdorf CS, White LR (1992) *J Chem Soc Faraday Trans II* 88:3576
19. Weast RC (1974) *CRC handbook of chemistry and physics*, 55th edn. CRC, Boca Raton
20. Alexander GB, Heston WM, Iler RK (1954) *J Am Chem Soc* 58:453
21. O'Brien RW, White LR (1978) *J Chem Soc Faraday Trans II* 74:1607
22. Foissy A, Persello J (1998) In: Legrand AP (ed) *The surface properties of silicas*. Wiley, Chichester, pp 365–414
23. Vogelsberger W, Löbbus M, Sonnenfeld J, Seidel A (1999) *Colloids Surf* 159:311
24. Tadros ThF, Lyklema J (1968) *J Electroanal Chem* 17:267
25. de Gennes P-G (1978) *J Phys Lett* 39:299
26. Wagner P, Brochard-Wyart F, Hervet H, de Gennes P-G (1993) *Colloid Polym Sci* 271:621
27. Garvey MJ, Tadros ThF, Vincent B (1974) *J Colloid Interface Sci* 49:57
28. Garvey MJ, Tadros ThF, Vincent B (1976) *J Colloid Interface Sci* 55:440
29. Baker JA, Pearson RA, Berg JC (1989) *Langmuir* 5:339
30. Ahmed MS, El-Aasser MS, Vanderhoff JW (1984) In: Goddard ED, Vincent B (eds) *Polymer adsorption and dispersion stability*. ACS Symposium Series 240. American Chemical Society, Washington, DC, pp 77
31. Kubota K, Fujishige S, Chu B (1992) *Macromolecules* 25:1618
32. Zhu PW, Napper DH (1996) *Langmuir* 12:5992
33. Tokuhiro T (1999) *J Phys Chem* 103:7097